ESR Studies of the Redox Orbitals in Diimine Complexes of Iron(II) and Ruthenium(II)

David E. Morris, Kenneth W. Hanck,* and M. Keith DeArmond*

Contribution from the Department of Chemistry, North Carolina State University, Raleigh, North Carolina 27650. *Received October 18, 1982*

Abstract: Variable-temperature ESR results are presented for the first three electrochemically generated reduction products of $[ML_3]^{2+}$ (M = Fe(II) and Ru(II), L = 4,4′-dimethyl-2,2′-bipyridine, 5,6-dimethyl-1,10-phenanthroline, and 2,2′-bipyridine) in fluid and frozen solutions of CH_3CN and DMF. In DMF solutions all of the Fe complexes decompose on the addition of one or more electrons, whereas the Ru complexes are stable toward addition of one and two electrons. The decomposition appears related to the greater coordinating ability of DMF relative to CH_3CN. All stable products that are soluble give ESR spectra typical of systems with ligand localized orbitals ($g \simeq 2.00$) and can be explained on the basis of an $S = {}^1/_2$ spin Hamiltonian. For all the singly reduced products and for the doubly reduced products in DMF a temperature-dependent variation in fluid solution line widths is interpreted as resulting from interligand electron hopping. The calculated activation barrier for hopping in the singly reduced products ($E_a \simeq (7\text{–}9) \times 10^2$ cm^{-1}) is twice that for the doubly reduced products. No line broadening is observed for the triply reduced products. For the doubly reduced products prepared in CH_3CN a broad, metal-centered signal is observed and interpreted to imply an electronic isomerization between metal-localized redox orbitals for the precipitated product and ligand-localized orbitals for the solution species. All results are consistent with and interpreted according to a single chelate ring localized redox orbital model that presumes isolated C_{2v} symmetry rather than molecular D_3 symmetry. In addition, the activation barriers to electron hopping are examined with regard to a vibronic coupling model for intramolecular electron-transfer processes.

Introduction

The intense interest in the spectroscopic and electrochemical properties of the nominally d^6 transition-metal imine complexes of general forms $[ML_3]^{n+}$, $[ML_2']^{n+}$, and $[ML_2X_2]^{n+}$ (such as $[Ru(bpy)_3]^{2+}$) is motivated primarily by the proven utility of several of these complexes in the photocatalytic water splitting process.[1-4] However, in spite of detailed photochemical studies of the lowest excited states, questions remain regarding the nature of the excited state[5-9] and redox[10] orbitals. Particularly significant to this report are questions concerning the spatial extent of the lowest unoccupied molecular orbitals[8] (the redox orbitals in electrochemistry and the charge-transfer (CT) excited-state orbitals in spectroscopy). While there is widespread agreement that these orbitals are predominantly ligand localized, there is still some question whether the orbitals are best described as multichelate ring delocalized (Figure 1A) with molecular D_3 symmetry in the case of $[ML_3]^{n+}$ or single chelate ring localized (spatially isolated, Figure 1B) with C_{2v} symmetry and a smaller amount of interligand interaction.

Compelling evidence for the single ring localization model for the redox orbitals in these complexes was obtained in recent work involving variable-temperature electron spin resonance (ESR) studies of the electrolytically generated reduction products of $[M(bpy)_3]^{2+}$[11] and $[M(terpy)_2]^{2+}$[12] (terpy = terpyridine; M = Fe(II) and Ru(II)). For the one- and three-electron reduced species in the tris complexes and the one- and two-electron reduced species in the bis complexes only $S = {}^1/_2$ behavior is observed. Further, for the singly reduced bipyridine complexes in fluid nitrile solvents, a temperature-dependent line broadening is observed, which is interpreted as resulting from an interligand electron-hopping phenomenon. From the line-broadening data, estimates of the magnitude of the energy barrier to hopping are reported. Thus, the observation of electron hopping between chelate rings and the absence of $S > {}^1/_2$ behavior for the species reduced by more than one electron are most easily rationalized by assuming single chelate ring (spatially isolated) redox orbitals.

The doubly reduced bipyridine complexes in the nitrile solvents appear to contradict the single ring localization model since ESR behavior characteristic of a more metal-localized redox orbital is observed.[11,13] However, the voltammetric pattern obtained for the parent ion and the heterogeneous electron-transfer rate constant data[14] for the second reduction step indicate that in CH_3CN solution the second electron also enters a ligand-localized redox orbital.

The single ring localization model predicts the availability of a ligand-localized orbital for the second electron as indicated by the molecular orbital diagram in Figure 2. In fact, a ligand-localized orbital should be energetically favored over a $d\sigma^*$ metal orbital. Thus, this apparent contradiction remains to be rationalized.

Additional support for single ring localized redox orbitals are recent reports from Elliott[15] and from Heath and co-workers[16,17] on the visible and near IR absorption spectra of some $[RuL_3]^{2+}$ reduction products. These spectra are dominated by $\pi\pi^*$ transitions of reduced and unreduced ligands whose intensities change in a regular manner with increasing extent of reduction. Such results are most easily explained by assuming distinct $L^{-\cdot}$ entities (i.e., $[Ru(bpy)_3]^+$ is best formulated as $[Ru(bpy)_2(bpy^-)]^+$). It also appears that the near IR bands for these complexes[15,17] are due to intervalence charge-transfer transitions, $L^{-\cdot} \rightarrow L$ (cf.

(1) Borgarello, E.; Kiwi, J.; Pelizzetti, E.; Visca, M.; Gratzel, M. *J. Am. Chem. Soc.* **1981**, *103*, 6324-6329.
(2) Sutin, N.; Creutz, C. *Pure Appl. Chem.* **1980**, *52*, 2717-2738.
(3) Dressick, W.; Meyer, T.; Durham, B.; Rillema, D. *Inorg. Chem.* **1982**, *21*, 3451-3458.
(4) Kalyanasundaram, K. *Coord. Chem. Rev.* **1982**, *46*, 159-244.
(5) Crosby, G. A. *Acc. Chem. Res.* **1975**, *8*, 231-238.
(6) Lacky, D. E.; Pankuch, B. J.; Crosby, G. A. *J. Phys. Chem.* **1980**, *84*, 2068-2074.
(7) Felix, F.; Ferguson, J.; Gudel, H.; Ludi, A. *J. Am. Chem. Soc.* **1980**, *102*, 4096-4102.
(8) DeArmond, M. K.; Carlin, C. M. *Coord. Chem. Rev.* **1981**, *36*, 325-355.
(9) Carlin, C. M.; DeArmond, M. K. *Chem. Phys. Lett.* **1982**, *89*, 297-302.
(10) Vlcek, A. A. *Coord. Chem. Rev.* **1982**, *43*, 39-62 and references therein.
(11) Motten, A. G.; Hanck, K. W.; DeArmond, M. K. *Chem. Phys. Lett.* **1981**, *79*, 541-546.
(12) Morris, D. E. Hanck, K. W.; DeArmond, M. K. *J. Electroanal. Chem.*, in press.
(13) Tanaka, N.; Ogata, T.; Niizuma, S. *Bull. Chem. Soc. Jpn.* **1973**, *46*, 3299-3301.
(14) Saji, T.; Aoyagui, S. *J. Electroanal. Chem.* **1975**, *63*, 31-37.
(15) Elliott, C. M. *J. Chem. Soc., Chem. Commun.* **1980**, 261-262.
(16) Heath, G. A.; Yellowlees, L. J.; Braterman, P. S. *J. Chem. Soc., Chem. Commun.* **1981**, 287-289.
(17) Heath, G.; Yellowlees, L.; Braterman, P. *Chem. Phys. Lett.* **1982**, *92*, 646-648.

0002-7863/83/1505-3032$01.50/0

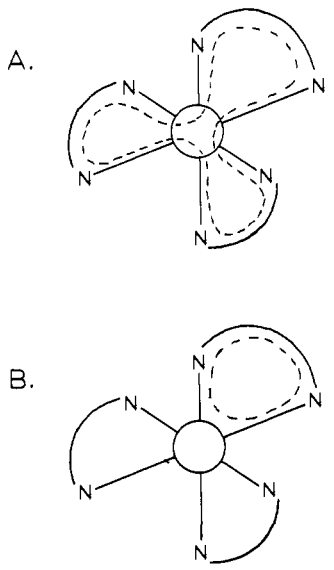

Figure 1. Spatial extent of lowest unoccupied molecular orbitals for d^6 tris(diimine) complexes: (A) multiring (D_3) delocalized; (B) single ring (C_{2v}) localized.

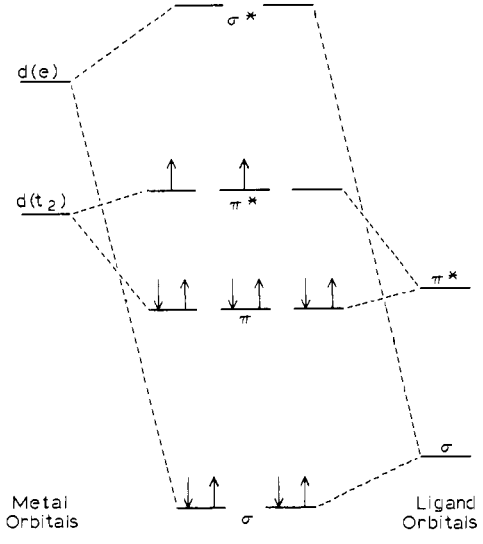

Figure 2. Suggested molecular orbital diagram for tris(diimine) complexes of d^6 transition metals. The configuration shown is the one expected for the doubly reduced reduction products where the π^* orbitals are single ring localized (one per ligand).

Creutz–Taube ion[18] and related mixed-valence complexes[19]). Such an assignment requires that there be a certain degree of charge localization.

Presuming the validity of Koopman's theorem for the parent ion, $[ML_3]^{2+}$, and the one-electron reduction product, these results also suggest that the CT excited-state orbitals for $[ML_3]^{2+}$ are single-ring localized. Such a conclusion is at odds with the interpretation of the spectroscopic data of Crosby and co-workers[5,6] and Felix et al.[7] in which D_3 symmetry is invoked to describe the orbital from which luminescence occurs. However, consistent with the single-ring description of these optical orbitals are the observations of multiple emissions from mixed-ligand Rh(III) complexes,[20] excited-state resonance Raman data for $[Ru(bpy)_3]^{2+}$,[21] and high-resolution photoselection data for a number of $[ML_3]^{2+}$ complexes,[9] all of which imply that the symmetry must be lower than D_3, most likely C_{2v}.

Table I. Half-Wave Potentials for Complex Redox Steps in 0.1 M Supporting Electrolyte[a]/DMF

	$E_{1/2}$, V vs. SSCE				
	+3/+2[b]	+2/+1	+1/0	0/−1	−1/−2
$[Fe(Me_2\text{-bpy})_3]^{2+}$	+0.930	−1.373	−1.552	−1.807	−2.25[c]
$[Fe(Me_2\text{-phen})_3]^{2+}$	+1.054	−1.299	−1.470	−1.714	−2.17[c]
$[Fe(bpy)_3]^{2+}$[d]		−1.26	−1.44	−1.70	−2.43
$[Fe(terpy)_2]^{2+}$[e]	+1.09	−1.260	−1.406	−2.050	−2.40[c]
$[Ru(Me_2\text{-bpy})_3]^{2+}$	+1.165	−1.336	−1.514	−1.770	−2.57[c]
$[Ru(Me_2\text{-phen})_3]^{2+}$	+1.266	−1.288	−1.452	−1.710	−2.45[c]
$[Ru(bpy)_3]^{2+}$[d]		−1.25	−1.43	−1.68	−2.30
$[Ru(terpy)_2]^{2+}$	+1.264	−1.266	−1.510	−1.948	−2.35[c]

[a] $TBABF_4$ in this work, TBAP in ref 25. [b] Metal-centered oxidation. [c] Voltammetric peak potential at 1.0 V/s, no anodic wave present. [d] Reference 25. [e] CH_3CN solvent, ref 12.

As part of a comprehensive experimental effort to verify the existence of single chelate ring localized optical and redox orbitals for these d^6 metal complexes of imine ligands and better characterize the phenomena associated with this model (electron and exciton hopping and the barriers involved), we now report further variable-temperature ESR results for the reduction products of some substituted diimine complexes of Fe(II) and Ru(II). Particular emphasis is given to the doubly reduced products in an effort to clarify the redox orbital character of these species and thus unify the single-ring-localization interpretation for the first three reduction products in these complexes.

Experimental Section

Reagents. The ruthenium complexes were prepared from $RuCl_3 \cdot nH_2O$ (Engelhard Industries) and the iron complexes from $Fe(NH_4)_2(SO_4)_2 \cdot 6H_2O$ (Baker and Adamson). The ligands 5,6-dimethyl-1,10-phenanthroline monohydrate (Me_2-phen) and 4,4′-dimethyl-2,2′-bipyridine (Me_2-bpy) were obtained from G. Frederick Smith and used without further purification. *N,N*′-dimethylformamide (Fisher Scientific) was purified by previously published procedures.[22] Acetonitrile (Gold Label, Aldrich Chemical) was used without further purification but was never exposed to noninert atmospheres. Tetraethylammonium perchlorate (Eastman Kodak) was recrystallized from water four times and dried in a vacuum oven prior to use. Tetrabutylammonium tetrafluoroborate (Electrometric Grade, Southwestern Analytical Chemicals) was used without further purification but dried in a vacuum oven prior to use.

Syntheses and Purification. The syntheses of $[Ru(Me_2\text{-phen})_3](PF_6)_2$ and $[Ru(Me_2\text{-bpy})_3](PF_6)_2$ were according to the same procedure described elsewhere[23] using a slight stoichiometric excess of ligand. $[Fe(Me_2\text{-phen})_3](PF_6)_2$ and $[Fe(Me_2\text{-bpy})_3](PF_6)_2$ were synthesized by the method of Musumeci et al.[24] for $[Fe(terpy)_2](ClO_4)_2$, again using a slight excess of ligand. All complexes were purified by repeated recrystallization from water/ethanol and/or acetone/water.

Apparatus and Procedure. The electrochemical apparatus for obtaining voltammetric data and carrying out bulk electrolyses has been described in detail elsewhere.[12] ESR samples were all prepared by ex situ electrolysis in either a vacuum line cell[11] or in a glovebox (Model HE 43-2, Vacuum Atmospheres) with a nitrogen atmosphere. Variable-temperature ESR spectra were recorded on a JEOL Co. X-band spectrometer equipped with a temperature controller.

Results

Electrochemistry. The cyclic voltammetric behavior of the $[ML_3]^{2+}$ complexes (M = Fe(II) and Ru(II), L = Me_2-bpy and Me_2-phen) is very similar to that observed for the corresponding tris(bipyridine) complexes. In all cases, a total of four redox steps are resolved in the available cathodic potential window in 0.1 M $TBABF_4/CH_3CN$. The voltammetric waves appear in a three-one pattern such that the spacings between the first three waves are approximately equal and much less than the spacing between the third and fourth waves. In addition, the first three waves are all reversible one-electron processes, whereas the fourth wave is irreversible at scan rates below about 20.0 V/s. Nearly identical behavior is also seen for all the complexes in DMF solutions. Table

(18) Creutz, C.; Taube, H. *J. Am. Chem. Soc.* **1969**, *91*, 3988–3989.
(19) Tanner, M.; Ludi, A. *Inorg. Chem.* **1981**, *20*, 2348–2350.
(20) Halper, W.; DeArmond, M. K. *J. Lumin.* **1972**, *5*, 225–237.
(21) Dallinger, R. F.; Woodruff, W. H. *J. Am. Chem. Soc.* **1979**, *101*, 4391–4393.
(22) Bezman, R.; Faulkner, L. *J. Am. Chem. Soc.* **1972**, *94*, 6317–6323.
(23) Segers, D.; DeArmond, M. K. *J. Phys. Chem.* **1982**, *86*, 3768–3776.
(24) Musumeci, S.; Rizzarelli, E.; Sammartano, S.; Bonomo, R. *J. Inorg. Nucl. Chem.* **1974**, *36*, 853–857.

Table II. g Values and Line Widths[a] for Complex Reduction Products in 0.1 M Supporting Electrolyte Solutions

	CH_3CN				DMF					CH_3CN			
	fluid[b]		frozen[c]		fluid[b]		frozen[c]			fluid[b]		frozen[c]	
	g	ΔH	g_{iso}	ΔH^d	g	ΔH	g_{iso}	ΔH^d		g	ΔH	g_{iso}	ΔH^d
RMB^+	1.994	54	2.000	18	1.996	52	2.002	16	FMB^+	1.994	64	1.997	15
RMB^0					1.996	28	2.002	17	FMP^+	1.990	120	1.994	17
RMB^-	1.995	28	2.001	18	1.993	15			FMP^0	2.15	~600		
RMP^+	1.990	73	1.998	32	1.991	72	1.995	52	FBY^{+h}	1.996	64	1.996	13
RMP^0	~2.3	~700			1.990	36[e]	1.993	47	FBY^{0h}	2.08			
RMP^-					1.987	30	1.99	~60	FBY^{-h}	1.995	12	1.997	12
RBY^{+f}	1.998	90	1.996	26			1.996	17	FTP^{+i}			1.982	36
RBY^{0f}	2.23	250			1.995	32	2.001	17	FTP^{0i}			1.983	34
RBY^{-f}	1.996	15	1.994	25									
RTP^{+g}			1.986	61			1.986	60					
RTP^{0g}			1.985	60			1.986	60					

[a] Peak to peak in gauss from derivative spectrum. [b] At room temperature ±10 °C except for Me_2-phen complexes, which are at 0 ± 5 °C. [c] At −120 ± 20 °C. [d] Calculated from $\Delta H = |H_\parallel - H_\perp|$. [e] Extrapolated value at 0 °C from lower temperature data. [f] $RBY^n = [Ru(bpy)_3]^n$; data from ref 11. [g] $RTP^n = [Ru(terpy)_2]^n$; data from ref 12. [h] $FBY^n = [Fe(bpy)_3]^n$; data from ref 11. [i] $FTP^n = [Fe(terpy)_2]^n$; data from ref 12.

I lists the $E_{1/2}$ values for the various redox steps in DMF. Data for the bis(terpyridine) complexes, whose electrochemical properties have been discussed in detail elsewhere,[12] and the tris(bipyridine) complexes have been included in Table I for comparison.

Controlled-potential electrolyses to produce the reduction products for subsequent spectroscopic investigation were carried out at potentials at least 50 mV cathodic of the respective voltammetric peaks. The postelectrolysis cyclic voltammetric technique discussed previously[12] was used to verify the identity and stability of the reduced species. In this way it was determined that neither of the iron complexes form stable reduction products in DMF solutions and that the products resulting from the addition of three electrons to the ruthenium complexes are unstable. No attempts were made to reduce any of the complexes by more than three electrons in either solvent.

For the iron complexes in DMF, the bulk electrolytic addition of one or more electrons results in the formation of a dark precipitate and a clear pink supernate within ~20 min after cessation of the reducing potential. Cyclic voltammetry of these solutions shows complete loss of all four of the parent ion cathodic waves. These results are consistent with the ligand dissociation process of other iron(II) di- and triimine complexes in organic solvents proposed by Van Meter and Neumann.[26]

According to this mechanism, the rate-determining step is the loss of one of the ligand molecules, followed by rapid loss of the remaining two. The ease of dissociation is related to both the solvent coordinating ability and its ability to solvate the dissociating ligand. Thus, for $[Fe(phen)_3]^{2+}$ the dissociative rate constant is ~100 times greater in DMF than in CH_3CN.[26] The cause of the apparent large enhancement in the rate of dissociation for the reduced species reported here is unknown, but it is likely related to the origin of the slight differences in the lowest unoccupied orbitals between the $[FeL_3]^{2+}$ and $[RuL_3]^{2+}$ complexes[27-30] since similar behavior is not observed for the ruthenium complexes until the third electron is added.

For the triply reduced ruthenium complexes in DMF the postelectrolysis voltammetry reveals that only two waves remain in the region of electroactivity of the parent complexes (Figure 3). These waves are shifted cathodically by a small amount with respect to the second and third waves of the unreduced species, and a new, irreversible oxidation wave appears at more anodic potentials. Although the valency of these reduction products is

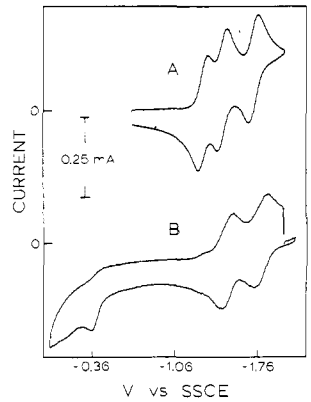

Figure 3. Cyclic voltammograms of (A) 0.9 mM $[Ru(Me_2\text{-phen})_3]^{2+}$ and (B) the same solution following exhaustive electrolysis at −1.990 V in 0.1 M TEAP/DMF. Scan rates are 1.0 V/s.

unknown, it is likely that their compositions are either $[RuL_2(solv)_2]^n$ or $[RuL_2(solv)L']^n$ (L = bidentate Me_2-bpy or Me_2-phen, L′ = monodentate Me_2-bpy or Me_2-phen, and solv = DMF).

The basis for these assignments are the known coordinating ability of DMF[26] and the electrochemical properties of similar species. In particular, the first two voltammetric waves of $[Ru(bpy)_2(CN)_2]^0$ correlate with the second and third waves of $[Ru(bpy)_3]^{2+}$ but with the peak potentials of the former shifted cathodically by a small amount.[31] Similarly, in the bisesquis complex, $[Ir(bpy)_2OH(bpy)]^{2+}$, the first two cathodic waves correlate with the second and third waves of $[Ir(bpy)_3]^{3+}$, again with a small cathodic shift relative to the tris complex.[32] Unfortunately, voltammetry alone is not able to distinguish between the two proposed compositions. The mechanism behind the partial or complete dissociation is likely related to the dissociation phenomenon observed for the iron complexes in DMF.

The only additional complication in the electrochemical generation of these reduction products is the very low solubility of the zerovalent (doubly reduced) species in CH_3CN solutions. For the $[FeL_3]^{2+}$ complexes every attempt to produce the $[FeL_3]^-$ species in a useful concentration is invariably thwarted by nearly quantitative precipitation of $[FeL_3]^0$. In addition, because solutions reduced at potentials corresponding to production of the doubly reduced species tend to precipitate $[ML_3]^0$ slowly (15–60 min, concentration dependent), it is impossible to determine whether the spectroscopic signals are due to solid species, solution species, or both.

ESR. For convenience in discussion, the reduction products are designated as follows: $[Fe(Me_2\text{-bpy})_3]^n$ = FMB^n; [Ru-

(25) Saji, T.; Aoyagui, S. *J. Electroanal. Chem.* **1975**, *58*, 401–410.
(26) Van Meter, F. M.; Neumann, H. M. *J. Am. Chem. Soc.* **1976**, *98*, 1388–1394.
(27) Creutz, C.; Chow, M.; Netzel, M.; Okumura, M.; Sutin, N. *J. Am. Chem. Soc.* **1980**, *102*, 1309–1319.
(28) DeLaive, P.; Foreman, T.; Giannotti, C.; Whitten, D. *J. Am. Chem. Soc.* **1980**, *102*, 5627–5631.
(29) Van Houten, J.; Watts, R. *J. Am. Chem. Soc.* **1976**, *98*, 4853–4858.
(30) Durham, B.; Walsh, J.; Carter, C.; Meyer, T. *Inorg. Chem.* **1980**, *19*, 860–865.
(31) Roffia, S.; Ciano, M. *J. Electroanal. Chem.* **1977**, *77*, 349–359.
(32) Kahl, J.; Hanck, K. W.; DeArmond, M. K. *J. Phys. Chem.* **1978**, *82*, 540–545.

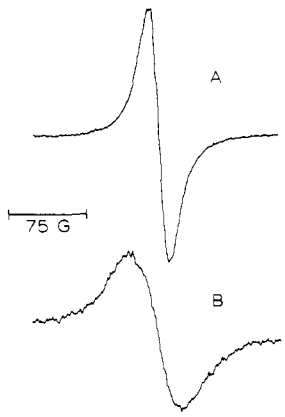

Figure 4. Fluid solution ESR spectra of (A) 1.0 mM $[Fe(Me_2\text{-bpy})_3]^+$ in 0.1 M $TBABF_4/CH_3CN$ and (B) 0.9 mM $[Fe(Me_2\text{-phen})_3]^+$ in 0.1 M $TEAP/CH_3CN$ (T = −43 °C).

Table III. Experimental g Shifts for the Complex Reduction Products in 0.1 M Supporting Electrolyte at ca. −150 °C

	CH_3CN		DMF	
	$\Delta g_\parallel$	$\Delta g_\perp$	$\Delta g_\parallel$	$\Delta g_\perp$
RMB^+	0.010	−0.001	0.007	−0.003
RMB^0			0.008	−0.003
RMB^-	0.009	−0.002		
RMP^+	0.018	−0.002	0.030	−0.002
RMP^0			0.028	−0.001
RMP^-			0.04	0.001
FMB^+	−0.001	0.009		
RBY^0			0.008	−0.002

$(Me_2\text{-bpy})_3]^n$ = RMB^n; $[Fe(Me_2\text{-phen})_3]^n$ = FMP^n; $[Ru(Me_2\text{-phen})_3]^n$ = RMP^n (n = 1+, 0, 1−). Table II contains the pertinent ESR parameters for the above reduction products together with the data for the reduction products of $[M(bpy)_3]^{2+}$ and $[M(terpy)_2]^{2+}$ (M = Fe(II) and Ru(II)) for comparison. All stable products are paramagnetic, giving ESR signals of comparable intensities.

The following are general trends in the ESR properties of the various species.

(1) With the exception of the doubly reduced species (n = 0) in CH_3CN, all reduction products give highly symmetric fluid solution signals in both solvents, and both fluid and frozen solution g values are very close to the free electron value, g_e = 2.0023.

(2) Except for minor variations in g values, the spectra for the products in fluid solutions are the same in DMF as in CH_3CN.

(3) The line widths for the fluid solution spectra of all the Me_2-phen products are 50% broader than those of the corresponding Me_2-bpy products throughout the fluid solution temperature range (Figure 4).

(4) The frozen solution signals for the ruthenium complexes are more asymmetric than those for the iron complexes, but the anisotropy (as measured by the g shifts, $\Delta g_{\parallel,\perp} = g_e - g_{\parallel,\perp}$) is small for all the reduction products (Table III). In addition, the parallel and perpendicular components are better resolved in frozen DMF solutions than in frozen CH_3CN solutions (Figure 5).

For all of the singly reduced species in fluid solutions of both solvents, a temperature-dependent line broadening is observed. These variations in line width (ΔH) are listed in Table IV together with the changes in the transverse or spin–spin relaxation times (T_2) to which the line widths correspond. For FMP^+ and RMP^+ the signals are too broad to easily distinguish the peaks from base-line noise at temperatures above ~0 °C. Thus, for these species, data are reported only for temperatures below 0 °C. For the triply reduced species (n = 1−) for which reliable preparations are possible (RMB^- and RMP^-), only small, random variations in the fluid solution line widths are observed.

The behavior of the doubly reduced products (n = 0) is complicated by their low solubility in CH_3CN. The majority of the experiments in which these zerovalent products are generated in

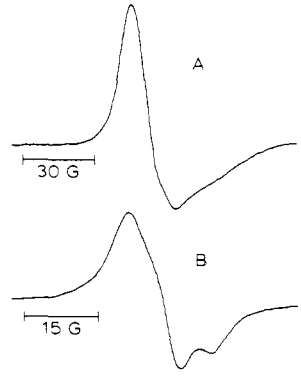

Figure 5. Frozen solution ESR spectra of $[Ru(Me_2\text{-bpy})_3]^+$: (A) 0.8 mM in 0.1 M $TBABF_4/CH_3CN$ (T = −105 °C); (B) 0.9 mM in 0.1 M $TBABF_4/DMF$ (T = −70 °C).

Table IV. Variations in Fluid Solution ESR Line Widths[a] and Relaxation Times for Complex Reduction Products

	high T[b]		low T[c]		
	ΔH, G	T_2, ns	ΔH, G	T_2, ns	solvent
RMB^+	54	7.7	19	22	CH_3CN
RMB^+	52	7.9	15	27	DMF
RMB^0	28[d]	15	16	26	DMF
RMP^+	77	5.3	36	11	CH_3CN
RMP^+	72	5.7	23	18	DMF
RMP^0	36	11	25	16	DMF
RBY^0	32[e]	13	17	23	DMF
FMB^+	64	6.4	18	22	CH_3CN
FMP^+	120	3.4	48	8.5	CH_3CN

[a] Peak to peak from derivative spectrum. [b] 25 ± 1 °C for Me_2-bpy complexes, 0 ± 1 °C for Me_2-phen complexes. [c] −41 ± 1 °C for CH_3CN solutions, −55 ± 1 °C for DMF solutions. [d] 6 °C. [e] 11 °C.

CH_3CN solution yield very broad ESR spectra (ΔH > 200 G) that have g values substantially shifted from the free electron value (Table II). However, in every instance that a broad spectrum is obtained, a precipitate can be detected in the sample tube on removal from the ESR cavity. In some cases, at very low concentrations (~0.1 mM), a signal similar to those of the singly reduced products (i.e., narrow width with $g \simeq 2$) or a superposition of broad and narrow signals is observed.

In DMF solutions, RMB^0 and RMP^0 are soluble (the iron complexes decompose), and for these species the ESR spectra have narrow line widths with g values similar to those of the singly reduced products. In fluid DMF solutions, the line widths of these species are temperature dependent (Table IV) although the magnitude of the variation of ΔH is considerably less than for RMB^+ and RMP^+. The same behavior is also observed for $[Ru(bpy)_3]^0$ in DMF.

No fine structure or forbidden (ΔM_s = 2) transitions typical of systems with $S > {}^1/_2$ were observed for any of the products reduced by two or more electrons in either solvent. In addition, no resolution of ^{14}N hyperfine structure (as was reported in the earlier study[11]) was obtained for any of the species in the present study.

Discussion

The most significant result of the present study is the observation of narrow ESR lines with $g \simeq 2.00$ for the doubly reduced products in DMF solution. Such findings are consistent with the occupation of ligand-localized π^* redox orbitals by the reduction electrons. This behavior is in contrast to that observed previously for these zerovalent species in CH_3CN (and in cases where the solid could be isolated), from both Tanaka's labs[13] and our labs.[11] In these earlier studies, broad ESR lines with substantial g shifts were reported and interpreted to imply that the redox orbitals for these products have much more metal orbital character. However, the results of Tanaka and co-workers were obtained by electrolysis at a mercury electrode at which they noted substantial precipi-

tation. As discussed earlier, in the present work at platinum electrodes in CH_3CN solutions, precipitation of the doubly reduced species invariably occurs, and in all cases where the broad signal is observed, some precipitate can be detected. In DMF solutions there is no evidence of precipitation of the zerovalent products, and the ESR parameters obtained in these cases are in excellent agreement with those of the other soluble reduction products (Table II).

The two distinctly different ESR responses for the doubly reduced products, one associated with a solution species and the other with a solid species, suggests that a type of electronic isomerization exists for these products. Namely, in solution the electrons are in ligand-localized orbitals, whereas in the solid the electrons occupy much more metal-localized orbitals. Such a description is consistent with the observed ESR behavior. The solution species give rise to spectra that are nearly identical with those of the other soluble reduced products ($g \simeq 2.00$ and relatively narrow lines) and are characteristic of ligand π^* redox orbitals. The solid species give spectra with much broader lines and substantial g shifts, both of which are characteristic of electrons in redox orbitals with a substantial amount of metal d orbital parentage.

The existence of this electronic isomerization between ligand-localized and metal localized orbitals is supported by electronic spectroscopic data for the parent (unreduced) ions that demonstrate that the energy difference between metal-centered and ligand-centered excited-state orbitals is small. In particular, the lowest excited state for the iron complexes is a metal-centered dd* state,[27] but there is a dπ^* state (metal to ligand charge transfer) at only slightly higher energy.[28] For the ruthenium complexes the lowest excited state is dπ^*,[9] but photochemical evidence for a close-lying dd* state has been presented.[29,30]

Thus, although the voltammetric data (pattern and spacings of waves, half-wave potentials, and heterogeneous rate constants),[14] the ESR results presented here, and Heath's absorption data for the reduction products of $[Ru(bpy)_3]^{2+}$ in dimethyl sulfoxide[16,17] clearly indicate that the second reduction electron enters a ligand-localized orbital and remains there provided the product stays in solution, it appears that crystallization of the reduced product results in sufficient alterations in the energy level ordering to allow one or both electrons to enter the metal-localized orbital(s). While the mechanism responsible for such reordering is at present unknown, it seems likely that the solvent makes a major contribution. Large pockets exist between the ligands in these complexes,[33] thus in solution the solvent molecules within these pockets may stabilize the ligand orbitals relative to the metal orbitals. In the solid such a solvation effect is not possible, so the metal orbitals may become energetically favorable.

The possibility that the extreme broadening of the ESR lines is due only to a change in the rate of some inter- or intramolecular dynamic process or the intrinsic lifetime for a product that retains a ligand-localized configuration in the solid seems unlikely. The magnitudes of the g shifts ($\Delta g \simeq 0.1$–0.3) are much too large to be consistent with a ligand-localized π^* orbital occupation. In addition, the shifts for the ruthenium complexes are larger than those for the iron complexes as might be expected for metal-localized orbitals simply on the basis of the extent of spin–orbit coupling.

In agreement with previous work,[11,13] both the singly and triply reduced products of the complexes examined here give ESR spectra characterized by relatively narrow lines with $g \simeq 2.00$, once again indicating that the redox orbitals for these species are ligand localized. The data, together with the new results for the doubly reduced products in DMF, conclusively establish the nearly identical nature of the redox orbitals for the one-, two-, and three-electron reduction products. This is particularly well illustrated by the frozen solution data, where g values and line widths are practically invariant for all three products. It is also noteworthy that none of the products produced by the addition

(33) Hanazaki, I.; Nagakura, S. *Inorg. Chem.* **1969**, *8*, 648–654 and references therein.

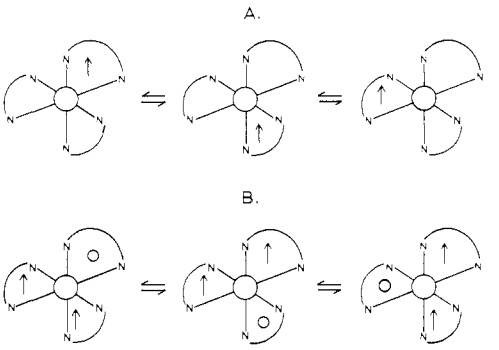

Figure 6. Pseudo-rotational hopping process: (A) singly reduced products with electron hopping; (B) doubly reduced products with hole hopping.

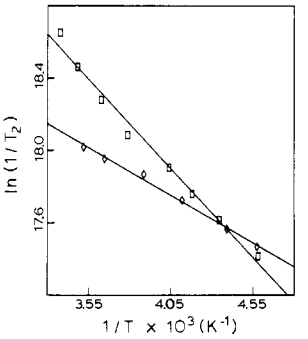

Figure 7. Arrhenius plots for $[Ru(Me_2\text{-}bpy)_3]^+$ (□) and $[Ru(Me_2\text{-}bpy)_3]^0$ (◇) in 0.1 M TEAP/DMF.

of two or more electrons shows any indication of $S > {}^1/_2$ behavior.

Clearly the most consistent rationale for these results is a single chelate ring localized redox orbital interpretation. This model predicts that each of the first three reduction electrons would enter one of the three spatially isolated, accidentally degenerate redox orbitals (Figure 2). Because these orbitals are single ring localized and inter-ring interactions appear to be very small, only $S = {}^1/_2$ behavior is observed for the species reduced by more than one electron. This implies that each of these three orbitals is, in essence, insulated from the other two so that, for example, the triply reduced product is best described as having three distinct, but equivalent, $S = {}^1/_2$ moieties.

Recently, it has been suggested[10] that a charge-localization model such as the one proposed here would lead to a 3-fold degenerate ground state for the singly reduced products, which would be in violation of the Jahn–Teller (JT) theorm. While this interpretation is possible for the one-electron products it does not seem to be consistent with the observed behavior of the other reduced species. The JT stabilization energy could not be large enough to favor spin pairing for the products with two or three electrons; therefore, a high spin configuration would be expected. However, such a picture would involve occupation of redox orbitals of slightly different energy (levels separated by JT stabilization energy) by the second and third electrons, likely producing a system with total spin $S > {}^1/_2$. The results presented here and previously[11-13] all indicate little, if any, difference in the orbital environments of the first-, second-, and third-reduction electrons, and there is definitely no indication that any of these species has $S > {}^1/_2$. This suggests that the redox orbitals are intrinsically single ring localized and only C_{2v} symmetry is applicable. Then, no orbital degeneracy exists, and JT distortions are not necessary to rationalize the results.

The electron-hopping phenomenon is probably the most unique and interesting manifestation of the proposed charge-localization model. As discussed previously,[11] this process can be treated as a pseudo spin–rotational coupling, which can be visualized for the singly reduced products as follows (Figure 6A): the electron, which is localized on one of the three ligand rings, can hop to either of the two vacant rings, thus simulating a 120° molecular rotation.

Table V. Activation Barriers for Electron Hopping

	E_a, cm^{-1}	solvent
RMB^+	750 ± 20	CH_3CN
RMB^+	690 ± 30	DMF
RMP^+	740 ± 30	CH_3CN
RMP^+	890 ± 50	DMF
RBY^{+a}	960 ± 50	CH_3CN
FMB^+	820 ± 20	CH_3CN
FMP^+	880 ± 10	CH_3CN
FBY^{+a}	960 ± 50	CH_3CN
RMB^0	370 ± 10	DMF
RMP^0	~300	DMF
RBY^0	440 ± 20	DMF

[a] Reference 11.

By analogy to normal spin–rotational coupling, such an interligand exchange process can be treated according to density matrix formalism, enabling the formulation of an Arrhenius expression[34] relating the spin–spin relaxation time to temperature. Therefore, a plot of ln $(1/T_2)$ vs. T^{-1} should be linear with the activation barrier to hopping given by the slope. Such a plot is shown in Figure 7 for RMB^+ in DMF, and the activation energies so obtained are tabulated in Table V. At present it cannot be determined whether the small variations in E_a for the singly reduced products are significant, but it bears noting that they are the of same magnitude and correspond to a vibrational quanta.

The doubly reduced products also show temperature-dependent line broadening in solution (Table IV). Although the magnitude of the line width variation is considerably less than for the one-electron products, linear fits to the Arrhenius equation are obtained as shown for RMB^0 in Figure 7. The acitvation energies for these products are included in Table V. These values are approximately a factor of 2 less than the corresponding values for the singly reduced species. This is a significant difference and suggests a fundamental change in intramolecular dynamics for the one- and two-electron products. In the single ring localization model, the doubly reduced products have an electron localized on two of the three ligand rings. Thus, this electron configuration corresponds to a *hole* in a half-filled manifold of orbitals. The difference in the magnitudes of the activation barriers for the one- and two-electron products likely reflects the difference between electron hopping (Figure 6A) and hole hopping (Figure 6B). This is not surprising since, while the mechanism of interligand electron (hole) exchange is likely the same, the energetic factors such as electron repulsion would certainly be altered.

For the triply reduced products no such line broadening is observed. However, this result is not inconsistent with the proposed interpretation. For these three-electron products there is one electron localized on each one of the three available ligand rings. In this case, the exchange would probably involve a momentary spin-pairing process that would greatly increase the energy barrier and make the total process energetically unfavorable.

Since charge localization and thermal charge-transfer processes are indicated for these reduced complexes, it is appropriate to examine these results with regard to the vibronic coupling model of Schatz et al.,[35,36] which has been successful in explaining charge localization and intramolecular charge transfer in a number of mixed-valence systems. Although this model has been rigorously developed only for the case of dimeric species such as the Creutz–Taube ion, the salient features should also apply to trimeric systems such as the tris(diimine) complexes considered here. In particular, for symmetric systems (i.e., those composed of a number of identical monomer units that differ only in their oxidation states), only two parameters are necessary to describe the interactions leading to charge localization. These are a vibronic term that tends to localize the orbital by coupling the energy of the electron with the energy of a particular vibrational mode and an exciton term that tends to delocalize the orbital through electronic coupling between the monomers.

The necessary criterion for charge localization is that the vibronic coupling be sufficiently greater than the exciton coupling so as to generate a ground-state potential-energy surface with multiple minima. However, for optical and thermal charge-transfer processes to occur, it is also necessary to have some nonzero value for the exciton coupling. The parameter of importance to this report is the ratio of the energy of the optical intervalence charge-transfer transition, E_{op}, to the energy of the activation barrier to thermal charge transfer, E_a. For strongly localized systems a lower limit of $E_{op}/E_a = 4$ is predicted. However, as the degree of exciton coupling increases, there is a concomitant increase in this ratio.[37]

In a recent report by Heath and co-workers,[17] it is suggested that the near-IR bands observed for the reduction products of $[Ru(bpy)_3]^{2+}$ are due to intervalence charge-transfer transitions. For both the one- and two-electron reduction products the maxima in these absorption spectra occur at 4500 cm^{-1}, while no absorption is detected in this region for the triply reduced product. These findings parallel those for the ESR line broadening due to interligand electron hopping reported here for the reduction products of $[Ru(bpy)_3]^{2+}$ and other complexes. In particular, the activation barrier to electron hopping for $[Ru(bpy)_3]^+$ ($E_a \simeq 1000$ cm^{-1}) is in excellent agreement with the predicted value of one-fourth of the optical transition energy. That the ratio of E_{op}/E_a for this species is slightly greater than the theoretical lower limit is an indication that there is some degree of exciton coupling between the ligands as required for the processes to occur.

The mechanism responsible for lowering the thermal barrier height in the doubly reduced products (E_a is only ~450 cm^{-1} for $[Ru(bpy)_3]^0$) cannot be completely explained at the present time. However, it is possible that the effect is due primarily to an increase in the exciton coupling. This would be consistent with the constant value reported for E_{op} in going from $[Ru(bpy)_3]^+$ to $[Ru(bpy)_3]^0$ since for localized systems E_{op} is independent of the extent of exciton coupling (ref 36, eq 14c), whereas E_a does depend on this quantity. It is also interesting that, in agreement with the absence of thermal charge transfer for the triply reduced products considered here, no optical transition is observed for $[Ru(bpy)_3]^-$.

Certainly, before quantitative conclusions regarding the extent of vibronic and exciton coupling in these reduction products can be made, it will be necessary to utilize a model that is rigorously applicable to trimeric systems. However, the vibronic coupling model considered here does offer the simplest framework within which the origin of charge localization and the occurrence of charge-transfer processes can be adequately described for this class of d^6 tris(diimine) complexes.

Summary and Conclusions

The variable-temperature ESR results presented here show that the redox orbitals of the reduction products resulting from the addition of one, two and three electrons to these nominally d^6 tris(diimine) complexes are nearly identical. In particular, the new ESR results for the doubly reduced products in DMF indicate that, in solution, the redox orbitals are ligand-localized types consistent with the interpretation of the cyclic voltammetric data (rate constant and pattern). These findings do suggest that the metal-centered redox orbitals identified by their characteristic ESR behavior both in this work and previously[11,13] result from species in the solid state that are electronic isomers of the ligand-localized solution species. Thus, in agreement with the photochemical results for the parent ions, the metal-localized and ligand-localized orbitals are nearly degenerate. The g values, effective spins (no $S > {}^1/_2$ spectra), and electron- (hole) hopping phenomenon can only be explained satisfactorily by a single chelate ring localized

(34) See ref 11, eq 3–7.
(35) Piepho, S. B.; Krausz, E. R.; Schatz, P. N. *J. Am. Chem. Soc.* **1978**, *100*, 2996–3005.
(36) Wong, K. Y.; Schatz, P. N.; Piepho, S. B. *J. Am. Chem. Soc.* **1979**, *101*, 2793–2803.

(37) For dimeric systems in the localized limit, $E_{op}/E_a = 2\lambda^2/[{}^1/_2\lambda^2 - |\epsilon| + (\epsilon^2/2\lambda^2)]$ (eq 16a, ref 36), where λ is the vibronic coupling term and ϵ is the exciton coupling term.

redox orbital model, which predicts the existence of three spatially isolated (intrinsically C_{2v}) portions of the molecular structure with, at most, minimal interaction. These conclusions are further substantiated by Heath's observation of the intervalence charge-transfer transitions in the reduction products of $[Ru(bpy)_3]^{2+}$, and both results appear consistent with the predictions of the vibronic coupling model of Schatz. Thus, a principal question remaining to be answered for the single ring model (both redox and optical orbitals) concerns the origin of the minimal interaction.

Acknowledgment. This research was supported by NSF Grant CHE-81-19702.

Registry No. $[Ru(Me_2\text{-phen})_3](PF_6)_2$, 85185-55-3; $[Ru(Me_2\text{-bpy})_3](PF_6)_2$, 83605-44-1; $[Fe(Me_2\text{-phen})_3](PF_6)_2$, 85202-31-9; $[Fe(Me_2\text{-bpy})_3](PF_6)_2$, 85185-57-5; FMP^+, 85185-58-6; FMP^0, 85185-59-7; FMB^+, 71619-84-6; RMB^+, 65605-26-7; RMB^0, 83605-52-1; RMB^-, 83605-53-2; RMP^+, 85185-60-0; RMP^0, 85185-61-1; RMP^-, 85185-62-2.

Synthesis and Characterization of the "Pocket" Porphyrins[1a]

James P. Collman,*[1b] John I. Brauman,*[1b] Terrence J. Collins,[1b] Brent L. Iverson,[1b] George Lang,*[1c] Roger B. Pettman,[1b] Jonathan L. Sessler,[1b] and Marc A. Walters[1d]

Contribution from the Department of Chemistry, Stanford University, Stanford, California 94305, the Department of Physics, Pennsylvania State University, University Park, Pennsylvania 16802, and the Department of Chemistry, Princeton University, Princeton, New Jersey 08540. *Received July 23, 1982*

Abstract: The synthesis of the "pocket" series is described. The iron(II) complexes have been extensively characterized by ^1H NMR, MCD, Mössbauer, direct axial ligand titrations, and magnetic susceptibility determinations. The results of these experiments indicate that in toluene, regimes of axial base concentration can be found in which iron(II) derivatives of the "pocket" porphyrins remain predominantly five-coordinate in the absence of gaseous ligand. Further, these five-coordinate complexes form stable and reversible oxygen adducts. The resonance Raman spectra of five-coordinate iron(II) "pocket" porphyrins are discussed as well as studies based on interactions with CO.

Recent attention has focused on developing synthetic iron(II) porphyrin complexes which are capable of reversibly binding O_2[2-6] in a manner analogous to hemoglobin (Hb)[7] and myoglobin (Mb). Many such models have been prepared[8-20] and their interactions with various ligands described.[14-25] To date, our own contributions

(1) (a) Abstracted from the Ph.D. thesis of J.L.S., Stanford University, 1982. (b) Stanford University. (c) Pennsylvania State University. (d) Princeton University.

(2) (a) Collman, J. P. *Acc. Chem. Res.* **1977**, *10*, 265-272. (b) Collman, J. P.; Halbert, T. R.; Suslick, K. S. In "Metal Ion Activation of Dioxygen"; Spiro, T. G., Ed.; Wiley: New York, 1980; Chapter 1.

(3) Jones, R. D.; Summerville, D. A.; Basolo, F. *Chem. Rev.* **1979**, *79*, 139-179.

(4) Wang, J.-H. *Acc. Chem. Res.* **1970**, *3*, 90-97.

(5) James, B. R. In "The Porphyrins"; Dolphin, D., Ed.; Academic Press: New York, 1978; Vol. V, pp. 206-301.

(6) Traylor, T. G. *Acc. Chem. Res.* **1981**, *14*, 102-109.

(7) Abbreviations: Hb(R), Hb(T) = relaxed and tense hemoglobin (human), respectively; Mb = myoglobin (sperm whale); $^{57}FeMb$ = apomyoglobin reconstituted with ^{57}Fe-enriched hemin. Fe-N_ϵ refers to the Fe-histidine F8 bond in Hb, and to the analogous Fe-imidazole (or py) bond in the models. K_B and $K_B{}^B$ refer to the equilibria constants for the binding of a single axial base to either the unligated or ligated iron(II) porphyrin complex. B = axial base; L = O_2 or CO; P = porphyrinato ligand; Im = imidazole; 1-MeIm = 1-methylimidazole; 2-MeIm = 2-methylimidazole; 1,2-Me_2Im = 1,2-dimethylimidazole; py = pyridine; H-Im-d_3 and H-Im-d_4 = triply and quadruply deuterated imidazole; py-d_5 = perdeuterated pyridine; 1-MeIm-d_6 = perdeuterated 1-methylimidazole; TPivP = "picket fence", *meso*-tetrakis($\alpha,\alpha,\alpha,\alpha$-*o*-pivalamidophenyl)porphyrinato; $Piv_3$5CIm = "tailed" "picket fence" = *meso*-tris(α,α,α-*o*-pivalamidophenyl)-β-*o*-5-(*N*-imidazolyl)valeramidophenylporphyrinato; $Piv_3$4CIm = "tailed" "picket fence" = *meso*-tris(α,α,α-*o*-pivalamidophenyl)-β-*o*-4-(*N*-imidazolyl)butyramidophenylporphyrinato; PF3Cu(py) = "pyridine-tailed" "picket fence" = *meso*-tris(α,α,α-*o*-pivalamidophenyl)-β-*o*-3-(3-pyridyl)propylureidophenylporphyrinato; C_5cap = "capped" = 5,10,15,20-[pyromellitoyl(tetrakis(*o*-oxyethoxyphenyl))]-porphyrinato; TPP = *meso*-tetraphenylporphyrinato; Fe-Cu-4, see ref 17; "chelated protoheme" = protoheme-*N*-[3-(1-imidazoyl)propyl]amide; PPIX = protoporphyrinato IX; PocPiv = "small" "pocket" = 5,10,15-((1,3,5-benzenetriyltriacetyl)tris(α,α,α-*o*-aminophenyl))-20-(α-*o*-pivalamidophenyl)porphyrinato, I; MedPoc = "medium" "pocket" = 5,10,15-(1,3,5-tris(benzenetripropionyl)tris(α,α,α-*o*-aminophenyl))-20-(α-*o*-pivalamidophenyl)porphyrinato, II; TalPoc = "tall" "pocket" = 5,10,15-(1,3,5-tris(benzenebutyryl)tris(α,α,α-*o*-aminophenyl))-20-(α-*o*-pivalamidophenyl)-porphyrinato, III; "doming" is the name given to the configuration in a five-coordinate metalloporphyrin in which the mean plane of the pyrrole nitrogens is different from that of the porphyrin; "ruffling" refers to a distortion of the porphyrin macrocycle toward D_{2d} geometry; cf. reg 36b.

(8) Chang, C. K.; Traylor, T. G. *J. Am. Chem. Soc.* **1973**, *95*, 5810-5811.

(9) (a) Collman, J. P.; Gagne, R. R.; Halbert, T. R.; Marchon, J. C.; Reed, C. A. *J. Am. Chem. Soc.* **1973**, *95*, 7868-7870. (b) Collman, J. P.; Brauman, J. I.; Doxsee, K. M.; Halbert, T. R.; Bunnenberg, E.; Linder, R. E.; LaMar, G. N.; DelGaudio, J.; Lang, G.; Spartalian, K. *Ibid.* **1980**, *102*, 4182-4192.

(10) (a) Baldwin, J. E.; Almog, J.; Dyer, R. L.; Peters, M. *J. Am. Chem. Soc.* **1975**, *97*, 226-227. (b) Almog, J.; Baldwin, J. E.; Huff, J. *Ibid.* **1975**, *97*, 227-228.

(11) (a) Battersby, A. R.; Buckley, D. G.; Hartley, S. G.; Turnbull, M. D. *J. Chem. Soc., Chem. Commun.* **1976**, 879-881. (b) Battersby, A. R.; Hamilton, A. D. *Ibid.* **1980**, 117-119.

(12) Baldwin, J. E.; Klose, T.; Peters, M. *J. Chem. Soc., Chem. Commun.* **1976**, 881-883.

(13) (a) Momenteau, M.; Rougee, M.; Loock, B. *Eur. J. Biochem.* **1976**, *71*, 63-76. (b) Momenteau, M.; Loock, B.; Mispelter, J.; Bisagni, E. *Nouv. J. Chim.* **1979**, *3*, 77-79.

(14) Momenteau, M.; Lavalette, D. *J. Chem. Soc., Chem. Commun.* **1982**, 341-343.

(15) (a) Traylor, T. G.; Stynes, D. V. *J. Am. Chem. Soc.* **1980**, *102*, 5938-5939. (b) Traylor, T. G.; Campbell, D.; Tsuchiya, S.; Mitchell, M.; Stynes, D. V. *Ibid.* **1980**, 5939-5941.

(16) Traylor, T. G.; Mitchell, M. J.; Tsuchiya, S.; Campbell, D. H.; Stynes, D. V.; Koga, N. *J. Am. Chem. Soc.* **1981**, *103*, 5234-5236.

(17) Ward, B.; Wang, C.-B.; Chang, C. K. *J. Am. Chem. Soc.* **1981**, *103*, 5236-5238.

(18) (a) Ellis, P. E., Jr.; Linard, J. E.; Szymanski, T.; Jones, R. D.; Budge, J. R.; Basolo, F. *J. Am. Chem. Soc.* **1980**, *102*, 1889-1896. (b) Linard, J. E.; Ellis, P. E., Jr.; Budge, J. R.; Jones, R. D.; Basolo, F. *Ibid.* **1980**, *102*, 1896-1904.

(19) Hashimoto, T.; Dyer, R. L.; Crossley, M. J.; Baldwin, J. E.; Basolo, F. *J. Am. Chem. Soc.* **1982**, *104*, 2101-2109.

(20) (a) A portion of this present work has appeared in preliminary form. Collman, J. P.; Brauman, J. I.; Collins, T. J.; Iverson, B.; Sessler, J. L. *J. Am. Chem. Soc.* **1981**, *103*, 2450-2452. (b) Results of gaseous ligand binding studies have been submitted for publication along with the present work. See: Collman, J. P.; Brauman, J. I.; Iverson, B. L.; Sessler, J. L.; Morris, R. M.; Gibson, Q. H., submitted for publication.

(21) (a) Brault, D.; Rougee, M. *Biochem. Biophys. Res. Commun.* **1974**, *57*, 654-659. (b) Brault, D.; Rougee, M. *Biochemistry* **1974**, *13*, 4591-4597. (c) Rougee, M.; Brault, D. *Ibid.* **1975**, *14*, 4100-4106.

(22) Collman, J. P.; Brauman, J. I.; Doxsee, K. M. *Proc. Natl. Acad. Sci. U.S.A.* **1979**, *76*, 6035-6039.

0002-7863/83/1505-3038$01.50/0